FEBS Letters 439 (1998) 26–30 FEBS 21088

Cloning and functional characterisation of the mouse $P2X_7$ receptor

I.P. Chessell[1,a,*], J. Simon[1,a,b], A.D. Hibell[a], A.D. Michel[a], E.A. Barnard[b], P.P.A. Humphrey[a]

[a] *Glaxo Institute of Applied Pharmacology, Department of Pharmacology, University of Cambridge, Tennis Court Road, Cambridge CB2 1QJ, UK*
[b] *Molecular Neurobiology Unit, Royal Free Hospital, London, UK*

Received 12 October 1998

Abstract We have isolated a 1785-bp complementary DNA (cDNA) encoding the murine $P2X_7$ receptor subunit from NTW8 mouse microglial cells. The encoded protein has 80% and 85% homology to the human and rat $P2X_7$ subunits, respectively. Functional properties of the heterologously expressed murine $P2X_7$ homomeric receptor broadly resembled those of the $P2X_7$ receptor in the native cell line. However, marked phenotypic differences were observed between the mouse receptor, and the other $P2X_7$ receptor orthologues isolated with respect to agonist and antagonist potencies, and the kinetics of formation of the large aqueous pore.

Key words: Mouse $P2X_7$ receptor; P2Z receptor; ATP; Pore

1. Introduction

P2X receptors are ligand-gated ion channels, which are activated by extracellular ATP. Their activation results in the opening of a non-selective cation channel with significant permeability to calcium [1,2]. In contrast to other P2X receptor subunits ($P2X_{1-6}$ [3]), the operational behaviour of $P2X_7$ is unique. Upon brief activation by agonist, the homomeric receptor acts as a non-selective cation channel. However, repeated or prolonged application of higher agonist concentrations, especially in solutions containing low concentrations of extracellular divalent cations, creates a much larger aqueous pore. Formation of this pore allows entry of fluorescent DNA binding dyes such as YO-PRO-1 (629 Da) and eventually leads to cell lysis. These same responses to ATP have been shown for native P2 receptors expressed by mast cells, macrophages or microglia and these receptors were previously referred to as P2Z receptors [4]. cDNAs encoding the rat and human $P2X_7$ receptor subunits have recently been isolated [1,2], and their pharmacological and electrophysiological properties, when they assemble homomeric channels, characterised. The characteristics of these $P2X_7$ receptor orthologues differ significantly from those of the $P2X_7$ receptor expressed endogenously in a mouse microglial cell line, NTW8 [5,6]. It was unclear whether these differences were conferred by species variation in the receptor sequence, expression level, or possible heteropolymerisation of the native $P2X_7$ receptor subunit with another subunit(s). Here we report isolation of a cDNA encoding the murine $P2X_7$ receptor from mouse NTW8 microglial cells, and show that its functional properties differ from rat and human $P2X_7$ recombinant receptors, when heterologously expressed in human embryonic kidney (HEK-293) cells.

2. Materials and methods

2.1. Isolation of cDNA encoding the murine $P2X_7$ receptor

The NTW8 mouse microglia cells were cultured to confluency as described [6]. Total RNA from these cells was extracted using a micro RNA isolation kit (Stratagene, Cambridge, UK), and was treated with RNase free DNase I (Stratagene) for 30 min at 37°C. First strand cDNA was synthesised (60 min, 42°C) from 10 μg of DNase treated total RNA using oligo$(dT)_{18}$ primer and Moloney murine leukemia virus reverse transcriptase (First Strand Synthesis Kit, Clontech, Palo Alto, CA, USA). A control reaction in the absence of reverse transcriptase was also carried out. The sequence specific primers based on the recently published rat $P2X_7$ cDNA sequence [1] were designed to amplify the entire coding sequence of the murine orthologue of this subunit in a polymerase chain reaction (PCR). The primers were as follows: forward primer, 5′-ATGCCGGCTTGCTGCAGCTGGAACGATGTCTTT-3′; reverse primer, 5′-TCAGTAGGGATACTTGAAGCCACTGTACTGCCC-3′. PCR amplifications were performed on 2 μl of first strand reaction using forward and reverse primers (200 ng each), 200 μM of each deoxynucleotides, 1.5 mM $MgCl_2$ in the presence of 2.5 units of AmpliTaq Gold DNA polymerase (PA Applied Biosystems, Warrington, UK). Cycling parameters were: 95°C, 9 min for 1 cycle; 94°C, 1 min, 57°C, 1 min, 72°C, 3 min for 35 cycles, with a final extension at 72°C for 10 min. The PCR reactions were then analysed by agarose gel electrophoresis. A single product was isolated and cloned into pCR 2.1 vector (TA Cloning kit, Invitrogen, Leek, The Netherlands) according to the manufacturer's instructions. Ten clones were sequenced completely using an automated DNA sequencer. For functional expression of the receptor, murine $P2X_7$ cDNA was subcloned into pcDNA 3.1(−) mammalian expression vector at the *Not*I-*Hin*dIII sites to give the correct orientation for transcription. The identity and orientation of the resulting clones were verified by sequencing.

2.2. Heterologous expression

1×10^6 wild-type HEK-293 cells, shown previously to be devoid of expressed endogenous P2X receptors [1,7], were transfected with 5 μg murine $P2X_7$ cDNA plasmid construct, using an electroporator (Easy-Ject, EquiBio, Kent, UK). Transfected cells were then selected in complete media (DMEM; Gibco-BRL, Paisley, UK) containing 10% foetal bovine serum (Gibco-BRL) and 500 μg/ml geneticin sulfate (G418; Gibco-BRL) for stable expression of the murine $P2X_7$ receptor, and passaged when confluent using standard methods.

2.3. Electrophysiological recordings

Recordings from HEK-293 cells transfected with mouse, rat [1] or human [2] $P2X_7$ receptor cDNA were made essentially as described [6]. Briefly, cells were perfused with extracellular solution, consisting of (in mM): NaCl 145, KCl 2, $CaCl_2$ 0.5, HEPES 10, D-glucose 10 (pH 7.3, osmolarity 300 mOsm), and whole cell patch-clamp recordings [8] were made with electrodes (resistance 2–5 MΩ) filled with (in mM): Cs aspartate 145, EGTA 11, HEPES 5, NaCl 2 (pH 7.3, osmolarity 290 mOsm). Currents were filtered with a corner frequency of 1–5 kHz (8-pole Bessel filter), digitised at 2–10 kHz using a Digidata 1200A (Axon Instruments, CA, USA) interface, and stored on computer. Data was only obtained from cells with a residual series resistance of less than 18 MΩ, and compensation for series resistance was used (>75%). Cells were voltage-clamped at −90 mV, unless otherwise stated. For voltage-ramp experiments, reported voltages were

*Correspondence author. Fax: (44) (1223) 334178.
E-mail: ic44126@glaxowellcome.co.uk

[1] These authors contributed equally to this work.

PII: S0014-5793(98)01332-5

corrected for the junction potential between the internal solution and the extracellular solution in which zero current was obtained before forming a seal. All experiments were performed at room temperature (22–24°C). Concentration-effect curves to ATP and 2′- and 3′-*O*-(4-benzoylbenzoyl)-adenosine 5′-triphosphate (BzATP; Sigma, Poole, UK) were determined by application of agonists to naive cells for 2 s using a computer controlled fast-flow U-tube system [9]. EC_{50} values were derived using a 3 parameter logistic equation (GraphPad Prism, CA, USA). Current augmentation [6] was studied by repeated application of 1 mM ATP (for 1 s every 20 s), up to 30 times. Current-voltage relationships were determined by performing a voltage ramp, over a 500-ms time course, from −75 to +60 mV holding potential, in the absence and presence of 100 μM BzATP.

2.4. YO-PRO-1 uptake

Uptake of the DNA binding dye, YO-PRO-1 (Molecular Probes, OR, USA) was performed essentially as described [10]. Confluent NTW8 or HEK-293 cells, stably expressing the recombinant murine, rat [1] or human [2,7] $P2X_7$ receptors were harvested, washed with ice-cold phosphate buffered saline (PBS) and centrifuged at 250×*g* for 5 min. The supernatant was discarded and the cells washed once in assay buffer consisting of (in mM): sucrose 280, HEPES 10, *N*-methyl-D-glucamine (NMDG) 5, KCl 5.6, glucose 10, $CaCl_2$ 1 (pH 7.4). YO-PRO-1 influx was initiated by the addition of 100 μl of cell suspension to 50 μl YO-PRO-1 (1.4 μM) and agonist mixture in assay buffer, and was performed in 96-well polystyrene 1/2 area flat bottom plates (Costar, Bucks, UK) at 37°C. The effects of 1-(*N,O*-bis[5-isoquinolinesulfonyl]-*N*-methyl-L-tyrosyl)-4-phenylpiperazine (KN-62), and pyridoxal-phosphate-6-azophenyl-2′,4′-disulfonic acid (PPADS) were studied by pre-incubation of cells for 20–30 min prior to addition of YO-PRO-1 and agonist; the effects of this agent were also studied on HEK-293 cells expressing the human recombinant $P2X_7$ receptor [7]. Reactions were terminated by centrifugation of the plates at 200×*g* for 5 min. Fluorescence was measured using a plate reader (Canberra-Packard, FluoroCount, Berks, UK) with an emission wavelength of 530 nm and an excitation wavelength of 485 nm.

3. Results

3.1. Isolation of the mouse $P2X_7$ cDNA

RT-PCR performed on mouse microglial total RNA produced a single 1785-bp product using specific primers based on the rat $P2X_7$ DNA sequence (Fig. 1). Sequencing revealed a single open reading frame corresponding to a protein of 595 amino acids (Fig. 2). The encoded protein showed a high degree of homology to the recently cloned human and rat $P2X_7$ subunits (80 and 85% identity, respectively), confirming its identity as a species orthologue of this P2X subunit (Fig. 2). However, this identity is less than that found for species orthologues of other P2X subunits (88–95% [11,12] and J. Simon, unpublished observation). The divergence in the amino acid sequence among the three species occurs predominantly in the extracellular loop and in the long C-terminal tail region, suggesting that subtle differences in the agonist potency and the kinetics of the pore formation could be expected (Fig. 2).

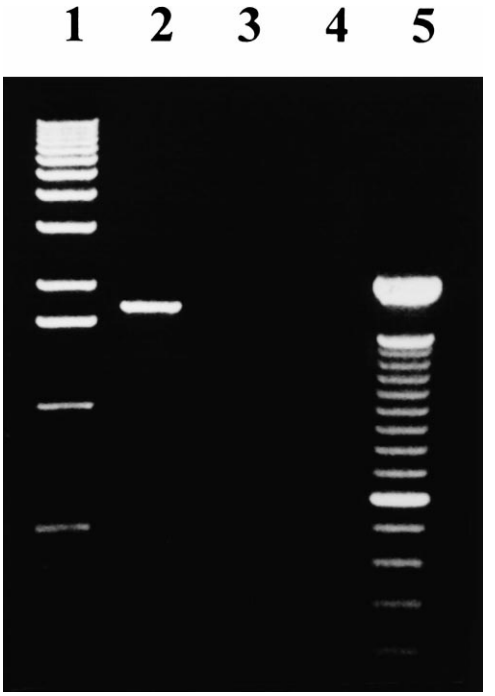

Fig. 1. Agarose gel electrophoresis of PCR amplification from cultured NTW8 mouse microglia cells. The gel (1%) was stained with ethidium bromide. Lane 1: 1-kb and lane 5: 100-bp DNA ladder (Gibco-BRL); Lane 2: PCP amplification product obtained from first strand cDNA using the rat $P2X_7$ specific primers. The band (1810 bp) corresponds to the predicted size of the mouse $mP2X_7$ cDNA-coding region. Lanes 3 and 4 are control reactions performed either in the absence of reverse transcriptase in the first strand reaction (lane 3) or in the absence of DNA template during the PCR amplification (lane 4). The PCR amplifications were repeated at least 3 times from different RNA preparations.

3.2. Functional studies

In low divalent cation-containing solution, BzATP and ATP evoked whole-cell inward currents (at a holding potential of −90 mV) in all mouse $P2X_7$-transfected HEK-293 cells tested, with BzATP being more potent than ATP. Brief applications of agonists produced concentration-effect curves with

Table 1
Pharmacological characteristics of native mouse $P2X_7$ receptor (NTW8) in comparison to recombinant $mP2X_7$, $hP2X_7$, and $rP2X_7$ receptors

	$mP2X_7$	NTW8	$hP2X_7$	$rP2X_7$
Electrophysiology				
BzATP EC_{50} (μM)	90.4 (70.4–116.2)	58.3 (46.1–73.9)	52.4 (36.3–75.6)	2.2 (1.7–2.9)
ATP EC_{50} (μM)	734 (707–762)	298 (255–347)	779 (372–1631)	220 (142–234)
YO-PRO-1 uptake				
BzATP EC_{50} (μM)	17.3 (14.8–20.2)	4.6 (4.1–5.3)	0.47 (0.67–0.59)	0.072 (0.062–0.083)
ATP EC_{50} (μM)	214 (176–259)	46.5 (40.3–53.7)	ND	ND
PPADS IC_{50} (μM)	9.0 (7.5–11.0)	7.0 (5.4–9.0)	0.015 (0.012–0.019)	0.087 (0.07–0 .11)
KN-62 IC_{50} (nM)	180 (120–253)	1170 (210–1120)	11 (8–18)	> 3000[a]

Top two rows: EC_{50} data obtained from electrophysiological experiments, from cells voltage clamped at −90 mV. Rows 3 and 4: EC_{50} values derived from YO-PRO-1 experiments. Rows 5 and 6: antagonist data obtained from YO-PRO-1 uptake experiments. Data is geometric mean with 95% confidence intervals, obtained from at least 6 determinations.
[a]See [15].

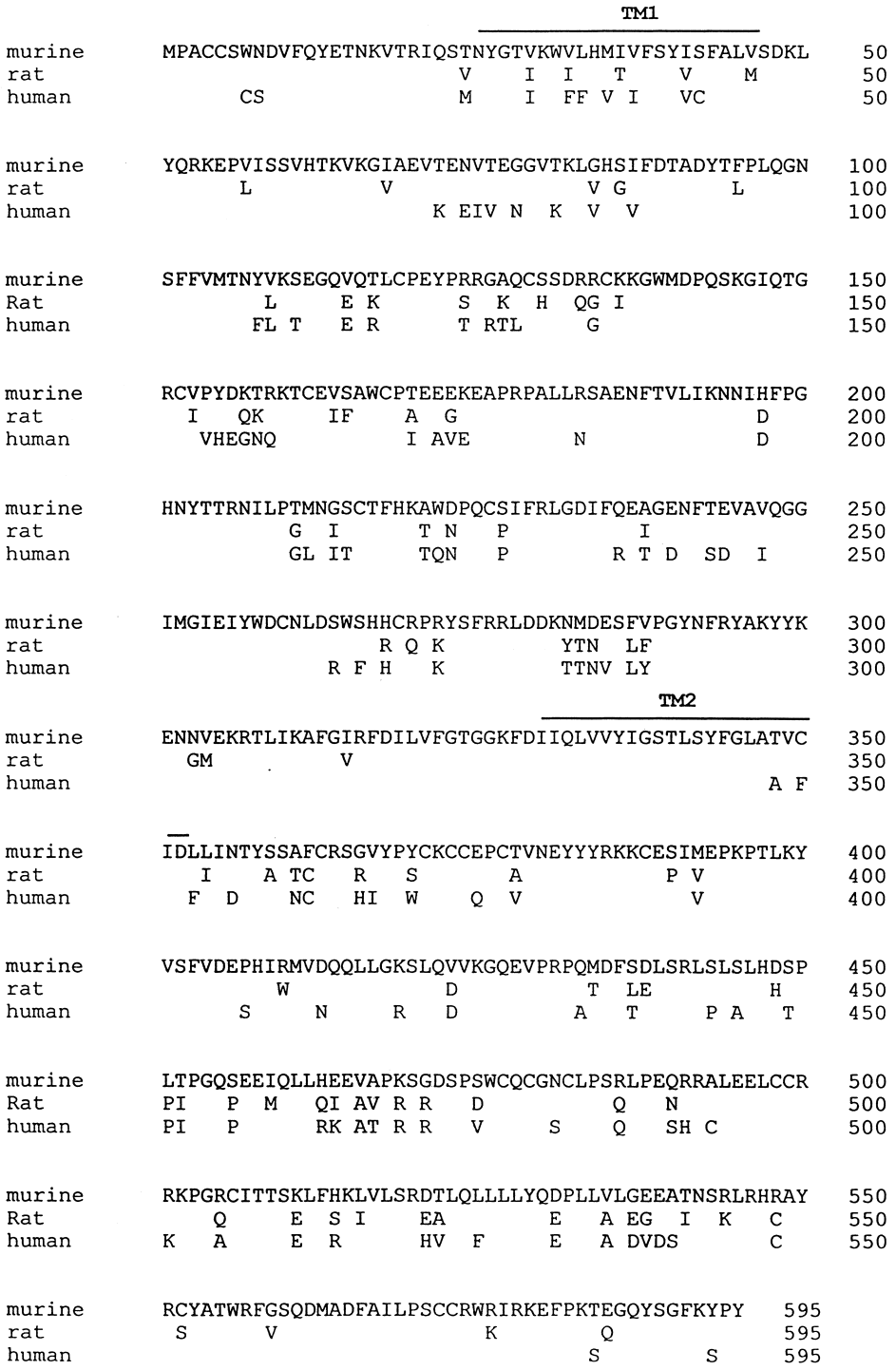

Fig. 2. Alignment of the predicted amino acid sequence of the mP2X$_7$ subunit from NTW8 cells with the rat (1) and human (2) mP2X$_7$ subunits. Overlined and marked as TM1 and TM2 indicate the predicted hydrophobic transmembrane segments. Amino acids shown for the human and rat mP2X$_7$ subunits indicate the difference in the sequence among the species orthologues. DNA sequence of the mP2X$_7$ subunit has been deposited in the EMBL database (accession number: AJ009823). Accession numbers for the rat and human mP2X$_7$ orthologues at the EMBL database are as follows: X95882 (rat) and Y9561 (human).

estimated EC_{50} values of 164.3 (89.3–302.2) μM and 1700 (900–3100) μM (BzATP, $n = 17$ and ATP, $n = 21$, respectively, geometric means with 95% confidence intervals; Fig. 3), and respective maximal inward currents of 1126 ± 227 pA and 1070 ± 116 pA. Current-voltage relationships generated with 1 mM ATP reversed at −2.6 mV, and did not display marked rectification (data not shown). Repeated applications of 1 mM ATP, for 1 s, produced currents that were successively larger, such that the 20th application produced a current which was 261.1 ± 43.5% of the 1st application current (8th application data shown in Fig. 4). Rise times and decay times for these currents did not change significantly over the application pro-

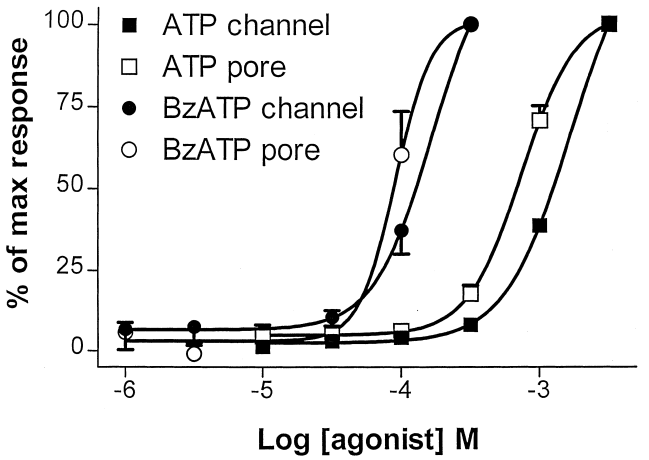

Fig. 3. Concentration-effect curves to ATP (■ and □) and BzATP (● and ○) in naive cells (closed symbols), and cells previously exposed to multiple applications of 1 mM ATP (reflecting the 'pore formed' state of the receptor; open symbols). All data was obtained from HEK293 cells expressing the mouse recombinant $P2X_7$ receptor, and are means ± S.E.M from at least 6 determinations.

tocol (Fig. 4). By analogy to the experiments in NTW8 microglial cells (Fig. 4, [6]), this current augmentation is thought to reflect formation of the 'large pore' characteristic of the $P2X_7$ receptor. Concentration-effect curves (Fig. 3) generated following this pore-formation procedure yielded EC_{50} values for BzATP and ATP of 90.4 (70.4–116.2) μM, $n=6$, and 734.6 (707.2–762.8) μM, $n=15$, respectively, which were not significantly different from EC_{50} values derived before the pore formation process (Table 1). Maximal inward currents were 2150 ± 218 and 3866 ± 683 pA (BzATP and ATP, respectively). Repeated applications of BzATP to cells expressing either the rat or human $P2X_7$ receptor revealed a different phenotype (Fig. 4). The amplitude of currents evoked by successive BzATP applications did not alter significantly over 8 applications, but the time taken for the inward currents to return to baseline values progressively increased (Fig. 4). This contrasts markedly to the phenotype of the recombinant and NTW8 $P2X_7$ receptors, where current amplitudes increased, but deactivation time was unchanged.

3.3. YO-PRO-1 uptake

The uptake of this DNA binding dye, reflecting large pore activation, was studied in HEK-293 cells, expressing the mouse $P2X_7$, and in the native NTW8 cell line. For both cell types, ATP and BzATP caused a concentration-dependent uptake, with BzATP being a more potent agonist than ATP (Fig. 5, Table 1). The increased potency of these agonists compared to that seen in electrophysiological recordings is attributable to differences in buffer composition [10]. BzATP was a more potent agonist at the rat and human recombinant orthologues of $P2X_7$ (see Table 1). The isoquinoline derivative, KN-62, inhibited BzATP-induced YO-PRO-1 influx in a concentration-dependent manner, and showed similar potency at both the recombinant mouse $P2X_7$ receptor and at NTW8 cells (Table 1). By comparison, KN-62 was a more potent antagonist at the human recombinant $P2X_7$ receptor, and was almost inactive at the rat recombinant $P2X_7$ receptor (Table 1). In addition, marked differences in the sensitivity to the non-selective P2 antagonist, PPADS, were observed between the murine $P2X_7$ receptors, and the human and rat recombinant receptors (Table 1).

4. Discussion

We have isolated a cDNA encoding the murine $P2X_7$ subunit from the NTW8 mouse microglial cell line, which is known to express $P2X_7$ [6]. The operational characteristics of recombinant homomeric channels formed by this $P2X_7$ subunit, when expressed heterologously, are similar to those observed in cells endogenously expressing mouse $P2X_7$, but differ markedly from other orthologues (rat and human) of this receptor.

The potencies of the agonists, ATP and BzATP, in both electrophysiological and YO-PRO-1 uptake studies, were similar for the cloned $mP2X_7$ receptor, and those observed for the natively-expressing NTW8 cells [6] with less than fivefold differences in relative potencies for each agonist. As expected, marked differences in agonist potencies were observed between experiments performed using electrophysiological recording and YO-PRO-1 uptake, which is attributable to the absence of sodium and chloride ions in the latter experiments [10]. In studies where current augmentation (thought to reflect

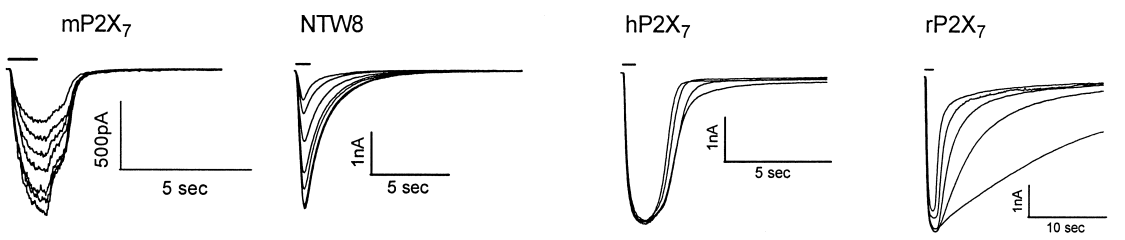

	mP2X7	NTW8	hP2X7	rP2X7
% increase 1st to 8th current 95-5% deactivation time	−12±11	39±44	145±44*	1259±451*
% increase 1st to 8th current amplitude	74±13*	303±60*	39±22	-7±10

Fig. 4. Representative traces of inward currents evoked by BzATP in cells expressing murine, rat and human $P2X_7$ receptors. Numerical data indicates the change in 95–5% deactivation time after 8 successive applications of BzATP (% increase), and the change in the inward current amplitude over the same application protocol (% increase). Note the striking phenotypic differences of current augmentation and deactivation kinetics between murine, rat and human receptors. Numerical data is mean ± S.E.M. (dotted line) of at least 8 determinations.

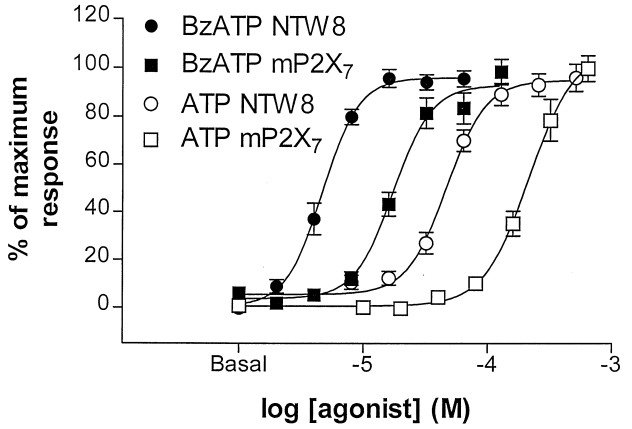

Fig. 5. Concentration-effect curves for agonist-induced YO-PRO-1 influx in NTW8 cells, and HEK293 cells expressing recombinant murine $P2X_7$ receptors (mP2X7) for BzATP (closed symbols) and ATP (open symbols). Data is mean ± S.E.M. of at least 6 determinations.

'large pore' formation) was examined, the NTW8 cells appeared to undergo this process more rapidly, with a plateau (of approximately 300% increase over the first current magnitude) for inward currents being attained after 8 applications of 1 mM ATP. In the HEK-293 cells expressing the recombinant receptor, a well-defined plateau was not observed even after 20 applications of 1 mM ATP, with the overall current augmentation at this time being an increase of approximately 250% of the first application current, and approximately 75% after 8 applications. The reasons for these modest quantitative differences may be due to receptor expression levels in the respective cell lines, or perhaps reflect a contribution of other subunits to the channel assembly in the NTW8 cells. Indeed, RT-PCR analysis has revealed the presence of additional P2X subunits in this cell line (J. Simon, unpublished observations).

The operational behaviour of the heterologously expressed mouse $P2X_7$ receptor differs considerably from the human and rat orthologues in several ways. Thus, the growth in current observed with repeated agonist applications (for both the recombinant and natively-expressed receptor) contrasts markedly with the human and rat recombinant receptors, where no such phenomenon is seen (see Fig. 4; [1,2]). In addition, for both the rat and human receptors, alterations in deactivation kinetics with multiple agonist applications are observed, such that the time for the responses to return to baseline became successively longer [1,7]. By contrast, for the NTW8 and recombinant mouse receptors, this deactivation time remained constant over multiple agonist applications. This may be a reflection of the way in which the large pore is formed, and how rapidly pore closure occurs, with differing mechanisms between the rat and human and mouse orthologues of this receptor.

There were also considerable differences in ligand recognition between the murine $P2X_7$ receptor and the other recombinant orthologues. In YO-PRO-1 uptake experiments, BzATP was greater than 100-fold more potent at the rat receptor, and some 30-fold more potent at the human receptor. There are also marked differences in antagonist sensitivity. Thus the potency of the $P2X_7$ antagonist, KN-62 [13], is at least 10-fold greater at the human recombinant $P2X_7$ receptor than at the recombinant mouse $P2X_7$ receptor, and was almost ineffective at the recombinant rat $P2X_7$ receptor. Furthermore, PPADS, which was a potent antagonist at the human and rat recombinant receptors, was almost 100-fold less potent at both the native and recombinant mouse $P2X_7$ receptors. Similarly, calmidazolium, a potent antagonist at the rat $P2X_7$ receptor (IC_{50} of 13 nM [14]) produced little inhibition of the mouse $P2X_7$ receptor at a concentration of 1 μM (I.P. Chessell, unpublished observations).

In summary, the cloning of the mouse $P2X_7$ receptor will allow further characterisation of this mechanistically intriguing receptor, and comparison of the various orthologues of this receptor should aid the understanding of the mechanism of channel to 'large pore' transition, characteristic of $P2X_7$ receptors.

References

[1] Surprenant, A., Rassendren, F., Kawashima, E., North, R.A. and Buell, G. (1996) Science 272, 735–738.
[2] Rassendren, F., Buell, G., Virginio, C., North, R.A. and Surprenant, A. (1997) J. Biol. Chem. 272, 5482–5486.
[3] Buell, G., Collo, G. and Rassendren, F. (1996) Eur. J. Neurosci. 8, 2221–2228.
[4] Di Virgilio, F. (1995) Immunol. Today 16, 524–528.
[5] Anderson, I.K., Choudry, S., Waslidge, N. and Rupniak, H.T.R. (1997) Br. J. Pharmacol. 120, 272P.
[6] Chessell, I.P., Michel, A.D. and Humphrey, P.P.A. (1997) Br. J. Pharmacol. 121, 1429–1437.
[7] Chessell, I.P., Michel, A.D. and Humphrey, P.P.A. (1998) Br. J. Pharmacol. 124, 1314–1320.
[8] Hamill, O.P., Marty, A., Neher, E., Sakmann, B. and Sigworth, F.J. (1981) Pflügers Arch. 391, 85–100.
[9] Fenwick, E.M., Marty, A. and Neher, E. (1982) J. Physiol. 331, 577–597.
[10] Michel, A.D., Hibell, A.D., Chessell, I.P. and Humphrey, P.P.A. (1997) Br. J. Pharmacol. 122, 113P.
[11] Valera, S., Talabot, F., Evans, R.J., Gos, A., Antonarakis, S.E., Morris, M.A. and Buell, G.N. (1995) Recept. Channels 3, 283–289.
[12] Garcia-Guzman, M., Soto, F., Gomez-Hernandez, J.M., Lund, P. and Stumer, W. (1997) Mol. Pharmacol. 51, 109–118.
[13] Gargett, C.E. and Wiley, J.S. (1997) Br. J. Pharmacol. 120, 1483–1490.
[14] Virginio, C., Church, D., North, R.A. and Surprenant, A. (1997) Neuropharmacology 36, 1285–1294.
[15] Humphreys, B.D., Virginio, C., Surprenant, A., Rice, J. and Dubyak, G.R. (1998) Mol. Pharmacol. 54, 22–32.